



## Fabrication electrospun GO/CS/PVA nanofibers and their application in dye-sensitized solar cells

Ngo Truong Ngoc Mai<sup>1</sup>, Ta Ngoc Don<sup>2</sup>, Nguyen Thi Quynh Hoa<sup>1</sup>, Nguyen Hong Ngoc<sup>1</sup>, Vien Vinh Phat<sup>1</sup>, Tran Thi Bich Quyen<sup>1</sup>, Dan-Thuy Van-Pham<sup>1</sup>, and Doan Van Hong Thien<sup>1\*</sup>

<sup>1</sup>Department of Chemical Engineering, Can Tho University–3/2 Street, Ninh Kieu District, Can Tho City, Vietnam

<sup>2</sup>Ministry of Education and Training, Hanoi, Vietnam

\*Email: [dvhthien@ctu.edu.vn](mailto:dvhthien@ctu.edu.vn)

### ARTICLE INFO

Received: 08/9/2021

Accepted: 28/9/2021

Published: 02/10/2021

#### Keywords:

Dye-sensitized solar cells, electrospinning, chitosan, PVA, graphene oxide, nanofibers

### ABSTRACT

In this study, graphene oxide (GO) was prepared by the Hummers method. GO/CS/PVA fibers were prepared by an electrospinning method. The structure, morphology and size of the electrospun materials were characterized by X – ray diffraction (XRD) and a scanning electron microscope (SEM). Fourier transformation infrared (FTIR) was used to confirm the formation of PVA/CS/GO. Raman spectroscopy was used to analyze the characteristic functional groups of carbon materials in GO. GO/CS/PVA nanofibers were successfully synthesized with an average diameter of about 108 nm and the bandgap energy was 3.2 eV. The nanofibers were used as a counter electrode for dye-sensitized solar cells. With the natural dye extracted from magenta leaves and the counter electrode based on GO/CS/PVA, the solar energy-to-electrical energy conversion efficiency was 0.65%.

### Introduction

The solar cell is produced with the purpose of replacing fossil fuels with renewable energy sources. The generation of electricity using solar energy has been the essence of scientific research, while the energy demand is increasing worldwide because of the rapid growth of the population [1, 2]. This challenge has to be answered with a low-cost issue using abundantly available raw materials. It is an important point that highlights the dye-sensitized solar cells (DSSC). Therefore, DSSC has emerged as one of the most promising alternatives to conventional silicon-based solar cells [3]. The DSSC technology is based on a nanostructured semiconductor photoanode (working electrode), photosensitizer, redox electrolyte, and a cathode (counter electrode). The efficiency of DSSC depends on not only the properties of the dye and

redox types of electrolytes but also the interaction between a working electrode and counter electrode.

The working electrode is based on semiconductor oxide with a wide band gap ( $\text{TiO}_2$ ,  $\text{ZnO}$ ,  $\text{SnO}_2$ ,  $\text{CeO}_2$ , and  $\text{Nb}_2\text{O}_5$ ) [4-8].  $\text{TiO}_2$  has been the most effective photoanode for many years. Nanocrystalline  $\text{TiO}_2$  with a high-surface-area-to-volume ratio is suitable for dye molecule absorption [8]. Many kind of  $\text{TiO}_2$  nanomaterials have been studied as working electrodes of DSSC [8].  $\text{TiO}_2$  materials are used for DSSC in the form of films, nanoparticles, nanorods, and nanofibers [9-12].

The counter electrode typically includes conductive TCO glass coated by a layer of catalyst. Platinum (Pt) is known to be an effective catalyst for DSSC [2, 13-15]. However, the use of Pt catalyst will make the cost of DSSC high. Recently, carbon-based materials,

conducting polymers, and polymer-carbon composites are potent substitutes for Pt-free counter electrodes of DSSC [16]. GO has been used as a catalyst for DSSC due to its versatile characteristics such as high surface-area-to-volume ratio, provided extra active sites, and good mechanical stability [17-19]. Composites (supported catalysts) are widely used for counter electrodes [18, 19]. Thus, the decoration GO with polymers would be a good choice for DSSC.

In this study, anthocyanin is extracted from the leaf of the magenta plant as a sensitizer for DSSC. Anthocyanin is the main component of several plants, flowers, fruits and gives efficient performances in photosensitization [20-22]. The mixture of chitosan (CS) and polyvinyl alcohol (PVA) were selected to disperse GO for electrospinning [23]. GO was synthesized by the Hummers method. The power conversion efficiency of DSSC was evaluated with the counter electrode of CS/PVA/GO nanofibers.

## Experimental

### Materials

Sulfuric acid ( $\text{H}_2\text{SO}_4$ ), acetic acid ( $\text{CH}_3\text{COOH}$ ), potassium iodide (KI), iodine ( $\text{I}_2$ ), titanium dioxide ( $\text{TiO}_2$ ), ethanol ( $\text{C}_2\text{H}_5\text{OH}$ ), PVA, CS, potassium permanganate ( $\text{KMnO}_4$ ), hydrogen peroxide ( $\text{H}_2\text{O}_2$ ) was purchased from Sigma. Sodium hydroxide (NaOH) and hydrochloric acid (HCl) were purchased from Merck. Fluorine doped tin oxide (FTO) coated glass substrates were purchased from Pilkington with a sheet resistance of  $15 \Omega/\text{square}$ . Distilled water was used for all of the experimental processes.

### Synthesized GO

GO was synthesized from coconut shell charcoal by Hummer's Modified method [24]. Briefly, coconut shell charcoal after milling was added in 4 M HCl solution for 3 hours with a weight ratio of 1:3 at  $45 \text{ }^\circ\text{C}$  to remove impurities. Then, the sample was washed with NaOH until pH neutral and dried for 24 h. Next, 1 g of coconut shell charcoal was added to 25 mL of concentrated  $\text{H}_2\text{SO}_4$  for 30 min at a temperature between  $0\text{-}20 \text{ }^\circ\text{C}$ . Then, 3 g of  $\text{KMnO}_4$  was slowly added to the above mixture and continued stirring for 25 min. The color of the solution changed to dark green and the temperature was still kept at  $0\text{-}20 \text{ }^\circ\text{C}$ . Then, 50 mL of deionized water was added slowly to the solution under stirring for 1 h. Next, 100 mL of

distilled water was added to the solution for another 15 min and then sonicated for 30 min. Later, 15 mL of 30% hydrogen peroxide was slowly added to the solution and stirred for 15 min to remove excess  $\text{KMnO}_4$  and then sonicated for 30 min. The mixture was then washed to neutral pH with a 5 M NaOH solution to obtain the final product (GO). Finally, GO was dried in an oven at  $60 \text{ }^\circ\text{C}$  for several days.

### Synthesized CS/PVA/ GO via an electrospinning method

CS solutions with different concentrations were dissolved in 3 wt% acetic acid at room temperature for 3 h. Next, the PVA with various contents was added in CS solution at  $80 \text{ }^\circ\text{C}$  under stirring for 5 hours to obtain the mixture. Then, GO was added to the mixture with 11% wt of GO under stirring for 1 hour to obtain the solution for electrospinning. The electrospinning experiments were carried out at the suitable conditions including: 14% of PVA concentration, 8/2 (wt/wt) of PVA/CS ratio,  $0.8 \text{ mL}\cdot\text{h}^{-1}$  of flow rate, 15 cm of tip-to-collector distance, 15 kV of applied voltage, and 11% wt of GO content.

### Materials characterization

X-ray diffraction (D8 Advanced Bruker, Germany) was used to determine the characteristic peaks, crystallinity and grain size of GO. The morphologies of GO/CS/PVA nanofibers were characterized by a scanning electron microscope (SEM, JSM-6390LV, JEOL, Japan). Fourier transform infrared (FTIR) spectroscopy (Nicolet 6700, Thermo Scientific) and Raman spectroscopy (XploRA ONE) were used to analyze the chemical structure and determine the functional groups present in the molecule, groups of carbon materials. UV/VIS spectrophotometer (UV-Vis, Pharo 300, Merck, Germany), was used to evaluate the bandgap energy.

### Fabrication of DSSC

5 g of magenta leaves were dried to saturated moisture content (about 3.3 wt%). Then, the dried magenta leaves were soaked in 30 mL of 50 wt% ethanol and 1 wt% HCl at  $40 \text{ }^\circ\text{C}$  for 1 h. FTO glass substrates with an effective area of  $1 \text{ cm} \times 1 \text{ cm}$  were washed with ethanol and cleaned using an ultrasonicator. For the preparation of photoanode, a FTO glass substrate was coated with  $\text{TiO}_2$  paste by the doctor blade technique and sintered at  $400 \text{ }^\circ\text{C}$  for 30

min. The FTO glass substrate with the TiO<sub>2</sub> layer was immersed in the extracted dye. For the counter electrode, the solution for electrospinning was prepared at proper conditions, including 14% of PVA concentration, 8/2 (wt/wt) of PVA/CS ratio, and 11% wt of GO content. FTO glass substrate that was cleaned previously was used as a collector for electrospinning. After electrospinning for 10 min, the PVA/CS/GO nanofibers were deposited on the FTO glass substrate. The counter electrode was treated by a thermal method at 200 °C for 15 min to remove the residue solvents. The electrolyte was prepared by mixing 0.83 g of potassium iodide and 0.127 g of iodine with 10 mL of ethylene glycol. The solution was stirred for 30 min at room temperature. DSSC was fabricated by sandwiching the working electrode and counter cathode. A micro syringe was used to inject the electrolyte into the middle of the electrodes. The J-V curve was obtained from the photoelectric measurement of the devices with an active area of 1 cm<sup>2</sup>.

## Results and discussion

### Characterization of GO

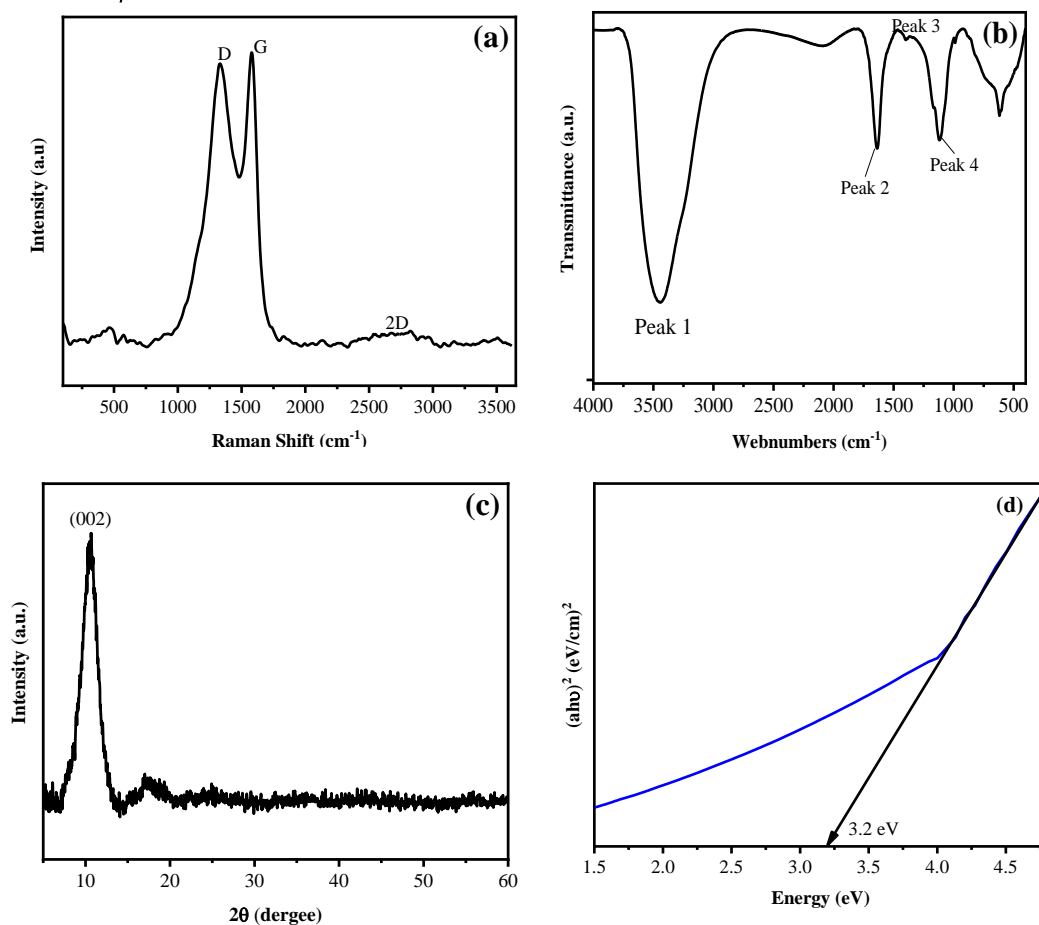


Figure 1a shows the Raman spectrum of GO. Two major peaks were observed, corresponding to D band (1350.9 cm<sup>-1</sup>) and G band (1585.7 cm<sup>-1</sup>), which are Raman characteristic peaks of GO. The peak of the G band corresponds to the sp<sup>2</sup> hybridized carbon in the graphitic lattice. The peak of D is related to defects or other impurities in the hybridized carbon. The intensity ratio of D-band to G-band (I<sub>D</sub>/I<sub>G</sub>) was 0.85. The results indicate the similarity of the I<sub>D</sub>/I<sub>G</sub> intensity ratio compared with previous reports [25, 26]. The 2D band is a crucial parameter for determining layer totals of the GO. Based on the intensity of 2D-band peak at 2758.8 cm<sup>-1</sup>, the synthesis of GO is multilayer [27, 28]. GO has been successfully synthesized.

Figure 1b shows the FTIR spectrum of GO. The oscillations extending from the hydroxyl groups (-OH) in the water molecule (-OH) were at peak 1 (3440.1 cm<sup>-1</sup>), the carboxylic functional group for peak 2 (1706.4 cm<sup>-1</sup>), the alcohol functional group for peak 3 (1399.9 cm<sup>-1</sup>) and epoxy functional group absorbed at wavelength 1119.9 cm<sup>-1</sup>. Therefore, the FTIR spectroscopy results confirm the formation of different functional oxygen-containing groups such as hydroxyl, carboxyl, alcohol and epoxy in the GO structure and

Figure 1: (a) Raman spectrum of GO; (b) FTIR spectrum of GO; (c) XRD patterns of GO; (d) Band gap energy of GO  
<https://doi.org/10.51316/jca.2021.076>

are similar to the FTIR spectroscopy for GO those reported by Leila [25] and Sujiono [26].

XRD pattern of GO sample in Figure 1c shows the (002) peak at the  $2\theta = 10.65^\circ$ . There are also peaks of impurities, but peak intensity is weak. According to Scherrer's equation, the distance between the stacking layers is 0.9 nm, the stacking height is 3.92 nm corresponding to 5 layers, which correspond to GO. The results follow the study of Leila [25].

The band gap energy of GO is 3.2 eV. This result indicates that coconut shell charcoal was originally an insulating material [26]. While the insulator has a bandgap energy of 5 eV and, after synthesis into a GO material, is a semiconductor with band gap energy lower 5 eV. The reduction in-band energy is due to the graphite powder's oxidation and the sample's acoustic variation. When compared with other studies such as synthesizing GO from coconut shell charcoal by the Hummer method of Sujiono [26] and Ji Chen [28], we found that the GO synthesized in this study has a smaller bandgap. This shows that GO synthesized from coconut shell charcoal by Hummer's Modified method is appropriate for the photosensitive solar cell applications.

#### Characterization of GO/CS/PVA nanofibers

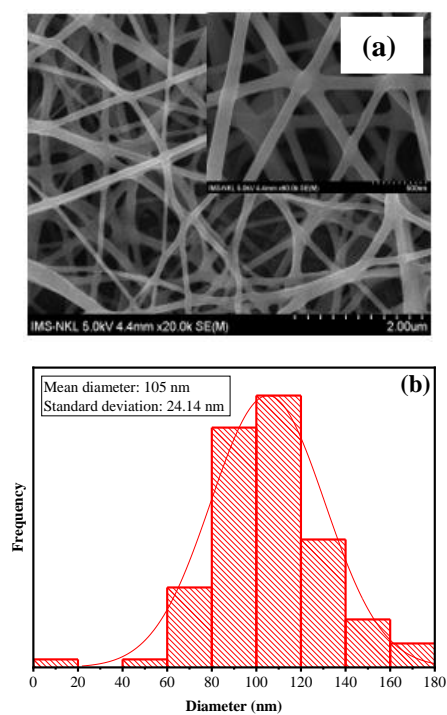


Figure 2: a) SEM images of GO/PVA/CS nanofibers; b) size distribution chart of GO

Figure 2a illustrates the SEM image of PVA/CS/GO fabricated at 14% wt of PVA concentration, PVA/CS ratio 8/2 (wt/wt), 11% wt of GO, 15 cm of tip-to-collector distance and 15 kV of applied voltage. It can be observed that nanofibers are uniform. Using ImageJ calculated average diameter of GO/CS/PVA nanofibers was  $105 \pm 24.14$  nm.

Figure 3 shows FTIR spectra of PVA (a); CS (b); GO (c), and GO/CS/PVA nanofibers (d). The characteristic peaks of CS, PVA and GO appeared. The peaks at  $1602\text{ cm}^{-1}$  and  $719\text{ cm}^{-1}$  indicate the presence of the amine group (N-H). The peak at  $1726\text{ cm}^{-1}$  represents the C=O bond of the carboxylic group. The broad and strong peak at  $3422\text{ cm}^{-1}$  corresponds to the OH stretching vibration. The sharp peak at  $2918\text{ cm}^{-1}$  is assigned to the asymmetric stretching of the  $-\text{CH}_2$  group.

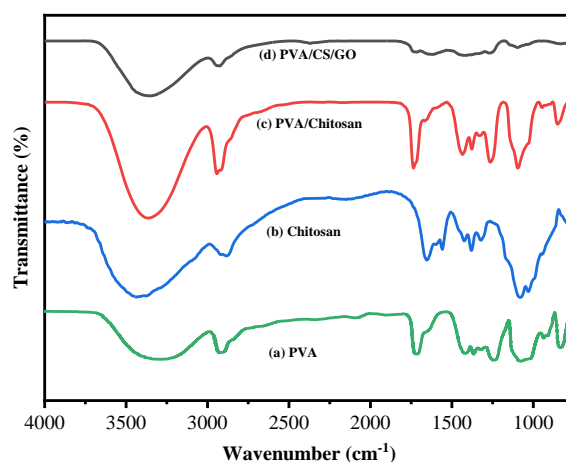


Figure 3: FTIR spectra of PVA (a); CS (b); GO (c), and GO/CS/PVA nanofibers (d).

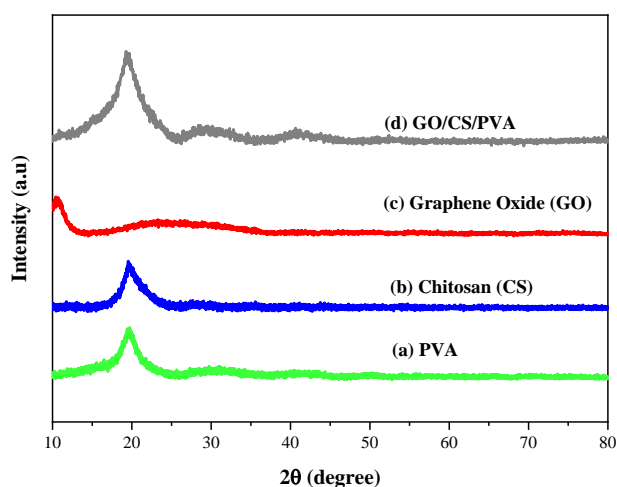


Figure 4: XRD patterns of PVA (a); CS (b); GO (c), and GO/CS/PVA nanofibers (d)

Figure 4 shows the X-ray diffraction (XRD) pattern of PVA, CS, GO and GO/PVA/CS nanofibers. Compared to pure CS, PVA, and GO, CS/PVA/GO nanofibers have three typical peaks at  $2\theta = 10.67^\circ$ ,  $19.7^\circ$ , and  $28^\circ$ . The peak at  $2\theta=19.7^\circ$  is the characteristic peak of PVA and CS [29]. The typical peak at  $2\theta=10.67^\circ$  corresponds to the (001) plane of GO. When CS and PVA molecules are in low interaction, CS or PVA has its own crystalline region, and the XRD curve can be observed as a simple mixing curve for CS and PVA. Thus, there were interactions among CS, PVA, and GO in the nanofibers.

### Photovoltaic performance

Main photovoltaic factors were determined including short-circuit photocurrent density ( $J_{sc}$ ), open-circuit voltage ( $V_{oc}$ ), fill factor (FF), maximum current density ( $J_{max}$ ), maximum voltage ( $V_{max}$ ), maximum power ( $P_{max}$ ), the intensity of the incident monochromatic light ( $I_{ins}$ ), and solar energy-to-electrical-energy conversion efficiency ( $\eta$ ). The current versus voltage curves were plotted. The solar energy-to-electrical energy conversion efficiency ( $\eta$ ) and fill factor (FF) were obtained from the equations:

$$FF = J_{max} \times V_{max} / J_{sc} \times V_{oc}$$

$$\eta(\%) = J_{sc} \times V_{oc} \times FF / I_{ins} \times 100$$

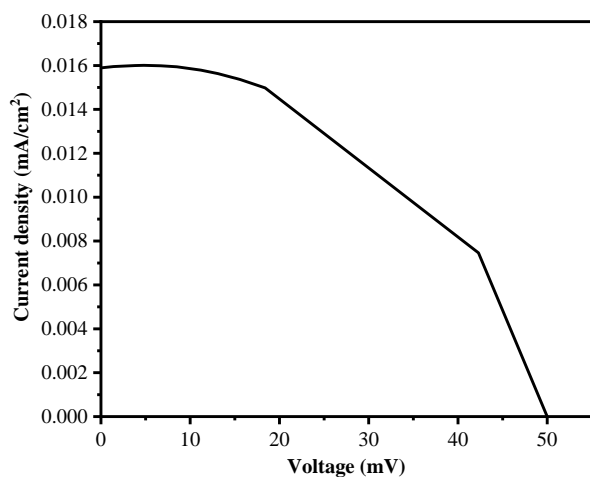


Figure 5: The J-V plot of DSSCs using PVA /CS/GO fibers with the dye of the leaf of magenta plant

Figure 5 depicts the J-V curves for the DSSC fabricated from the counter electrode of PVA/CS/GO nanofibers and a sensitizer extracted from the leaf of magenta. The open-circuit voltage ( $V_{oc}$ ) was 50 mV and the short circuit density ( $J_{sc}$ ) was 0.08 mA/cm<sup>2</sup>. From the J-V curve of DSSC, the maximum power point ( $P_{max}$ ) was evaluated corresponding to the photocurrent maximum ( $J_{max}$ ) and potential maximum ( $V_{max}$ ). In this study, the maximum  $P_{max}$  of 6.56 mW/cm<sup>2</sup>, the filling

coefficient of 1.71, and solar energy-to-electrical energy conversion efficiency ( $\eta$ ) of 0.65% were determined.

The solar energy-to-electrical energy conversion efficiency of fabricated DSSC with various natural dyes and counter electrodes are summarized in Table 1. When using the dye extracted from the leaf of magenta plant as a sensitizer, the efficiency was a little higher than that of the other natural dyes which use carbon as the catalyst. It may be because the interaction between anthocyanin within the dye with the surface of TiO<sub>2</sub>. With Pt catalyst, the efficiency obtained in this study was almost higher than that of previous studies for other types of natural dyes. Therefore, DSSC has been successfully fabricated with a natural photosensitizer extracted from magenta leaves and the counter electrode based on CS/PVA/GO nanofibers.

Table 1: Photovoltaic efficiency of DSSCs with various natural dyes and catalysts

Dye	Catalyst	Efficiency (%)	Ref.
Nasturtium flowers	Platinum	0.28	[30]
Citrus reticulata	Platinum	0.71	[31]
Red frangipani	Platinum	0.3	[32]
Rhododendron	Platinum	0.57	[33]
Shea	Carbon	0.25	[34]
Pereskia bleo	Carbon	0.11	[35]
Magenta leaves (this study)	GO/CS/PVA	0.65	

### Conclusion

GO was successfully synthesized from coconut shell charcoal by Hummer's Modified method and CS/PVA/GO nanofibers were fabricated by an electrospinning method. And they were characterized by SEM, XRD, and FTIR. CS/PVA/GO nanofibers were deposited on a FTO glass substrate as a counter electrode of DSSC while a natural dye extracted from magenta leaves was used as a sensitizer. The solar energy-to-electrical energy conversion efficiency from Pt-free counter electrode was 0.65%.

### Acknowledgments

This work was funded by the Vietnam Ministry of Education and Training, under grant number B2021-TCT-05.

## References

- J.J. Yoo, G. Seo, M.R. Chua, T.G. Park, Y. Lu, F. Rotermund, Y.-K. Kim, C.S. Moon, N.J. Jeon, J.-P. Correa-Baena, V. Bulović, S.S. Shin, M.G. Bawendi, and J. Seo. Efficient perovskite solar cells via improved carrier management, *Nature*, 590 (2021) 587-593.  
<https://10.1038/s41586-021-03285-w>.
- A. Hagfeldt, G. Boschloo, L. Sun, L. Kloo, and H. Pettersson. Dye-Sensitized Solar Cells, *Chemical Reviews*, 110 (2010) 6595-6663.  
<https://10.1021/cr900356p>
- M. Law, L.E. Greene, J.C. Johnson, R. Saykally, and P. Yang. Nanowire dye-sensitized solar cells, *Nature Materials*, 4 (2005) 455-459.  
<https://10.1038/nmat1387>
- A. Zatirostami. SnO<sub>2</sub>- based DSSC with SnSe counter electrode prepared by sputtering and selenization of Sn: Effect of selenization temperature, *Materials Science in Semiconductor Processing*, 135 (2021) 106044.  
<https://doi.org/10.1016/j.mssp.2021.106044>.
- M. Sufyan, U. Mehmood, Y. Qayyum Gill, R. Nazar, and A. Ul Haq Khan. Hydrothermally synthesize zinc oxide (ZnO) nanorods as an effective photoanode material for third-generation Dye-sensitized solar cells (DSSCs), *Materials Letters*, 297 (2021) 130017.  
<https://doi.org/10.1016/j.matlet.2021.130017>
- S.V. Umale, S.N. Tambat, and S.M. Sontakke. Combustion synthesized CeO<sub>2</sub> as an anodic material in dye sensitized solar cells, *Materials Research Bulletin*, 94 (2017) 483-488.  
<https://doi.org/10.1016/j.materresbull.2017.07.004>
- G. Taques Tractz, F. Staciaki da Luz, S. Regina Masetto Antunes, E. do Prado Banczek, M. Taras da Cunha, and P. Rogério Pinto Rodrigues. Nb<sub>2</sub>O<sub>5</sub> synthesis and characterization by Pechini method to the application as electron transport material in a solar device, *Solar Energy*, 216 (2021) 1-6.  
<https://doi.org/10.1016/j.solener.2021.01.029>
- A. Omar, M.S. Ali, and N. Abd Rahim. Electron transport properties analysis of titanium dioxide dye-sensitized solar cells (TiO<sub>2</sub>-DSSCs) based natural dyes using electrochemical impedance spectroscopy concept: A review, *Solar Energy*, 207 (2020) 1088-1121.  
<https://doi.org/10.1016/j.solener.2020.07.028>
- S. Shakir, H.M. Abd-ur-Rehman, R. Zahid, M. Iwamoto, and V. Periasamy. Multistep electrophoretic deposition of TiO<sub>2</sub> film and its surface modification for dye sensitized solar cells, *Journal of Alloys and Compounds*, 837 (2020) 155579.  
<https://doi.org/10.1016/j.jallcom.2020.155579>
- R. Selvapriya, V. Sasirekha, P. Vajeeston, J.M. Pearce, and J. Mayandi. Reaction induced multifunctional TiO<sub>2</sub> rod/particle nanostructured materials for screen printed dye sensitized solar cells, *Ceramics International*, 47 (2021), 8094-8104.  
<https://doi.org/10.1016/j.ceramint.2020.11.164>
- V. Madurai Ramakrishnan, S. Pitchaiya, N. Muthukumarasamy, K. Kvamme, G. Rajesh, S. Agilan, A. Pugazhendhi, and D. Velauthapillai. Performance of TiO<sub>2</sub> nanoparticles synthesized by microwave and solvothermal methods as photoanode in dye-sensitized solar cells (DSSC), *International Journal of Hydrogen Energy*, 45 (2020) 27036-27046.  
<https://doi.org/10.1016/j.ijhydene.2020.07.018>
- J. Sun, X. Yang, L. Zhao, B. Dong, and S. Wang. Ag-decorated TiO<sub>2</sub> nanofibers for highly efficient dye sensitized solar cell, *Materials Letters*, 260 (2020) 126882.  
<https://doi.org/10.1016/j.matlet.2019.126882>
- M.N. Mustafa and Y. Sulaiman. Review on the effect of compact layers and light scattering layers on the enhancement of dye-sensitized solar cells, *Solar Energy*, 215 (2021) 26-43.  
<https://doi.org/10.1016/j.solener.2020.12.030>
- M. Hamadani, J. Safaei-Ghomi, M. Hosseinpour, R. Masoomi, and V. Jabbari. Uses of new natural dye photosensitizers in fabrication of high potential dye-sensitized solar cells (DSSCs), *Materials Science in Semiconductor Processing*, 27 (2014) 733-739.  
<https://doi.org/10.1016/j.mssp.2014.08.017>
- V. Sugathan, E. John, and K. Sudhakar. Recent improvements in dye sensitized solar cells: A review, *Renewable and Sustainable Energy Reviews*, 52 (2015) 54-64.  
<https://doi.org/10.1016/j.rser.2015.07.076>
- J. Wu, Z. Lan, J. Lin, M. Huang, Y. Huang, L. Fan, G. Luo, Y. Lin, Y. Xie, and Y. Wei. Counter electrodes in dye-sensitized solar cells, *Chemical Society Reviews*, 46 (2017) 5975-6023.  
<https://doi.org/10.1039/C6CS00752J>
- A.A. Qureshi, S. Javed, H.M. Asif Javed, A. Akram, M. Jamshaid, and A. Shaheen. Strategic design of Cu/TiO<sub>2</sub>-based photoanode and rGO-Fe<sub>3</sub>O<sub>4</sub>-based counter electrode for optimized plasmonic dye-sensitized solar cells, *Optical Materials*, 109 (2020)

110267.  
<https://doi.org/10.1016/j.optmat.2020.110267>
18. A. Singh, D. Poddar, S. Thakur, and R. Jha. Ternary composite based on MoSe<sub>2</sub>-rGO/ polyaniline as an efficient counter electrode catalyst for dye sensitized solar cells, *Materials Chemistry and Physics*, 273 (2021) 125043. <https://doi.org/10.1016/j.matchemphys.2021.125043>
  19. J. Ma, S. Yuan, S. Yang, H. Lu, and Y. Li. Poly(3,4-ethylenedioxythiophene)/reduced graphene oxide composites as counter electrodes for high efficiency dye-sensitized solar cells, *Applied Surface Science*, 440 (2018) 8-15. <https://doi.org/10.1016/j.apsusc.2018.01.100>
  20. D. Sampaio, R.S. Babu, H. Costa, and A. De Barros. Investigation of nanostructured TiO<sub>2</sub> thin film coatings for DSSCs application using natural dye extracted from jaboticaba fruit as photosensitizers, *Ionics*, 25 (2019) 2893-2902. <https://doi.org/10.1007/s11581-018-2753-6>
  21. S.A. Mozaffari, M. Saeidi, and R. Rahmanian. Photoelectric characterization of fabricated dye-sensitized solar cell using dye extracted from red Siahkooti fruit as natural sensitizer, *Spectrochimica Acta Part A: Molecular and Biomolecular Spectroscopy*, 142 (2015) 226-231. <https://doi.org/10.1016/j.saa.2015.02.003>
  22. I.C. Maurya, P. Srivastava, and L. Bahadur. Dye-sensitized solar cell using extract from petals of male flowers *Luffa cylindrica* L. as a natural sensitizer, *Optical Materials*, 52 (2016) 150-156. <https://doi.org/10.1016/j.optmat.2015.12.016>
  23. D.V.H. Thien. Electrospun chitosan/PVA nanofibers for drug delivery, *Vietnam Journal of Science and Technology*, 54 (2016) 185-185. <https://doi.org/10.15625/2525-2518/54/4B/12040>
  24. M.S. Khan, R. Yadav, R. Vyas, A. Sharma, M.K. Banerjee, and K. Sachdev. Synthesis and evaluation of reduced graphene oxide for supercapacitor application, *Materials Today: Proceedings*, 30 (2020) 153-156. <https://doi.org/10.1016/j.matpr.2020.05.403>
  25. L. Shahriary and A.A. Athawale. Graphene oxide synthesized by using modified hummers approach, *Int. J. Renew. Energy Environ. Eng.*, 2 (2014) 58-63.
  26. E.H. Sujiono, D. Zabrian, M. Dahlan, B. Amin, and J. Agus. Graphene oxide based coconut shell waste: synthesis by modified Hummers method and characterization, *Heliyon*, 6 (2020) e04568. <https://doi.org/10.1016/j.heliyon.2020.e04568>
  27. W. Zhou, J. Zeng, X. Li, J. Xu, Y. Shi, W. Ren, F. Miao, B. Wang, and D. Xing. Ultraviolet Raman spectra of double-resonant modes of graphene, *Carbon*, 101 (2016) 235-238. <https://doi.org/10.1016/j.carbon.2016.01.102>
  28. Y. Ding, P. Zhang, Q. Zhuo, H. Ren, Z. Yang, and Y. Jiang. A green approach to the synthesis of reduced graphene oxide nanosheets under UV irradiation, *Nanotechnology*, 22 (2011) 215601. <https://doi.org/10.1088/0957-4484/22/21/215601>
  29. J. Shen, M. Shi, B. Yan, H. Ma, N. Li, and M. Ye. Ionic liquid-assisted one-step hydrothermal synthesis of TiO<sub>2</sub>-reduced graphene oxide composites, *Nano Research*, 4 (2011) 795. <https://doi.org/10.1007/s12274-011-0136-7>
  30. S. Singh, I.C. Maurya, S. Sharma, S.P.S. Kushwaha, P. Srivastava, and L. Bahadur. Application of new natural dyes extracted from *Nasturtium* flowers (*Tropaeolum majus*) as photosensitizer in dye-sensitized solar cells, *Optik*, 243 (2021) 167331. <https://doi.org/10.1016/j.jileo.2021.167331>
  31. E.C. Prima, N.N. Hidayat, B. Yulianto, Suyatman, and H.K. Dipojono. A combined spectroscopic and TDDFT study of natural dyes extracted from fruit peels of *Citrus reticulata* and *Musa acuminata* for dye-sensitized solar cells, *Spectrochimica Acta Part A: Molecular and Biomolecular Spectroscopy*, 171 (2017) 112-125. <https://doi.org/10.1016/j.saa.2016.07.024>
  32. V. Shanmugam, S. Manoharan, S. Anandan, and R. Murugan. Performance of dye-sensitized solar cells fabricated with extracts from fruits of ivy gourd and flowers of red frangipani as sensitizers, *Spectrochimica Acta Part A: Molecular and Biomolecular Spectroscopy*, 104 (2013) 35-40. <https://doi.org/10.1016/j.saa.2012.11.098>
  33. H. Zhou, L. Wu, Y. Gao, and T. Ma. Dye-sensitized solar cells using 20 natural dyes as sensitizers, *Journal of Photochemistry and Photobiology A: Chemistry*, 219 (2011) 188-194. <https://doi.org/10.1016/j.jphotochem.2011.02.008>
  34. U.I. Ndeze, J. Aidan, S.C. Ezike, and J.F. Wansah. Comparative performances of nature-based dyes extracted from Baobab and Shea leaves photosensitizers for dye-sensitized solar cells (DSSCs), *Current Research in Green and Sustainable Chemistry*, 4 (2021) 100105. <https://doi.org/10.1016/j.crgsc.2021.100105>
  35. S.M. Amir-Al Zumahi, N. Arobi, M. Mahbubur Rahman, M. Kamal Hossain, M. Ara Jahan Rozy, M.S. Bashar, A. Amri, H. Kabir, M. Abul Hossain, and F. Ahmed. Understanding the optical behaviours and the power conversion efficiency of novel organic dye and nanostructured TiO<sub>2</sub> based integrated DSSCs, *Solar Energy*, 225 (2021) 129-147. <https://doi.org/10.1016/j.solener.2021.07.024>  
<https://doi.org/10.51316/jca.2021.076>